ORIGINAL ARTICLE

Synthesis and properties of hyperbranched polymers by polymerization of an AB$_3$-type incompletely condensed cage silsesquioxane (IC-POSS) monomer

Sota Yuasa[1] · Hiroaki Imoto[1] · Kensuke Naka[1]

Abstract

An incompletely condensed cage silsesquioxane (IC-POSS)-based AB$_3$-type monomer, tris(dimethylsilyl)-*p*-vinylhexaisobutyl-IC-POSS (**3**), was prepared by the corner-cleaved reaction of vinylheptaisobutyl-POSS (**1**) and subsequent capping reaction with chlorodimethylsilane. The structure of **3** was confirmed by FT-IR; ^{1}H-, ^{13}C-, and ^{29}Si-NMR; and HR-FAB-MS analyses. These analyses also suggested 12.5 mol% contamination of tris(dimethylsilyl)-heptaisobutyl-IC-POSS (**4**). The hydrosilylation polymerization of **3** as an AB$_3$-type IC-POSS monomer in the presence of Karstedt's catalyst in toluene at 80 °C overnight provided a soluble polymer with a number average molecular weight (M_n) and molecular weight distribution (M_w/M_n) of the polymer that are 3.9×10^3 and 1.39, respectively. The resulting hyperbranched polymer (HB) reacted with two molar equivalents of isoprenol or allylheptaisobutyl-POSS against the Si–H groups in the presence of Karstedt's catalyst in toluene at 80 °C for 7 h. The HB polymers before and after post functionalization with isoprenol or allylheptaisobutyl-POSS showed 1% weight loss at 298, 285, and 358 °C, respectively, under N$_2$. Introducing POSS units at the terminus significantly increased the thermal stability. The XRD pattern of the HB polymers showed a denser structure formed in the allylheptaisobutyl-POSS-terminated HB polymer. The refractive index of the HB polymer before post functionalization was 1.4376. Post functionalization with isoprenol and allylheptaisobutyl-POSS increased the refractive index to 1.4464 and 1.4573, respectively.

Introduction

Many studies have examined hybrid polymers with cage silsesquioxane (POSS) units covalently bound to their structures, which lead to an enhancement in their physical properties, i.e., improved thermal and mechanical stability, flammability, oxidative resistance, and a low dielectric constant [1–7]. Among them, hyperbranched (HB) polymers have attracted much attention because of their interesting physical properties resulting from their highly branched architecture and their large number of terminal functional groups [8–11]. Compared with linear polymers, HB polymers possess considerably higher solubility, lower viscosity, and decreased inter-chain entanglement. The properties of

HB polymers are extremely dependent on the terminal functional groups and can be tailored by post functionalization. HB polymers with pendant [12–14] and terminal POSS units [15] have been prepared. POSS units at the terminal position provide crystalline HB polymers, resulting in nanoscale composite materials with well-defined architectures, although dendritic polymers are usually unable to crystallize due to their highly branched topology [15].

Polymers incorporating POSS units at the branched points are expected to possess significantly improved hydrophobicity, as well as show significantly reduced dynamics of the polymer segments, which leads to an increase in their glass-transition temperature [16–19]. HB polymers are synthesized through the self-polymerization of one A$_x$B$_y$-type monomer or via a nonlinear bimolecular polymerization using an A$_x$-type monomer and a B$_y$-type monomer. Cage octasilsesquioxanes (octafunctional-POSS) can be introduced into an HB architecture either as an A$_x$B$_y$-

✉ Kensuke Naka
kenaka@kit.ac.jp

1 Faculty of Molecular Chemistry and Engineering, Graduate School of Science and Technology, Kyoto Institute of Technology, Goshokaido-cho, Matsugasaki, Sakyo-ku, Kyoto 606-8585, Japan

type monomer (where x + y = 8) or as an A_x-type monomer. Almost all known octafunctional-POSS compounds synthesized to date have either eight identical functional groups or a seven–one configuration [20]. Octafunctional-POSS monomers and various difunctional silanes were subjected to bimolecular nonlinear A_8–B_2 polymerization to provide HB polycarbosilane and polysiloxanes [16]. However, a strict-feed molar ratio with a large excess of B-type monomer was implemented to avoid gelation, resulting in poor growth and structure control, as well as low yield and an additional purification step to remove excess B-type monomers. These HB polymers were functionalized with curable alkoxysilane-end groups to fabricate transparent and robust nanostructured POSS-containing coatings for use in a range of high-performance space and solar applications. We also reported that HB polymers with POSS-branching points were prepared by bimolecular nonlinear polymerization [21]. AB_7-type POSS monomers containing one thiol and seven vinyl groups were used to construct HB-POSS polymers with controlled growth [17]. Compared with A_8- and AB_7-type POSS monomers, POSS-based compounds with two functional groups have been seldom reported [22–34]. The hydrosilylation polymerization of a bifunctional double-decker-shaped silsesquioxane (DDSQ) as an A_2-type monomer and a dimethylsilyl-capped incompletely condensed cage silsesquioxane as an A_3-type monomer was reported [19]. However, the development of A_xB_y-type monomers based on well-defined POSS structures is still limited.

We recently developed a novel material design based on an incompletely condensed cage silsesquioxane (IC-POSS), in which one corner of the cubic backbone is open. IC-POSS architectures significantly reduce their crystallinity, but their thermal stability is comparable to those of completely condensed POSS architectures [35, 36]. We also found that the selective corner-opening of vinylheptaisobutyl-POSS (**1**) occurs under appropriate conditions [37]. The subsequent corner-capping of the resulting trisilanol vinylhexaisobutyl-IC-POSS (**2**) afforded *para*-substituted bisvinylhexaisobutyl-POSS as an A_2-type monomer [37]. Trisilanol vinylhexaisobutyl-IC-POSS (**2**) is an effective candidate for an AB_3-type monomer to create an HB architecture. Here, we prepared tris(dimethylsilyl)-*p*-vinylhexaisobutyl-IC-POSS as an AB_3-type IC-POSS monomer and used it for hydrosilylation polymerization to obtain HB polymers.

Experimental procedures

Materials

Tetrahydrofuran (THF), triethylamine (Et$_3$N), methanol (MeOH), *n*-hexane, and anhydrous magnesium sulfate (MgSO$_4$) were purchased from Nacalai Tesque (Kyoto,

Japan). Distilled water, tetrahydrofuran (THF, super dehydrated grade), and toluene (super dehydrated grade) were purchased from Wako Pure Chemical Industry, Ltd. (Osaka, Japan). A xylene solution (0.1 M) of platinum(0)-1,3-divinyl-1,1,3,3-tetramethyldisiloxane (Pt(dvs)) and a tetra-ethylammonium hydroxide solution (35 wt% in H$_2$O) were purchased from Sigma-Aldrich Japan (Tokyo, Japan). Chlorodimethylsilane and 3-methyl-3-buten-1-ol (isoprenol) were purchased from Tokyo Chemical Industry (Tokyo, Japan). Vinylheptaisobutyl-POSS [14] and allylheptaisobutyl-POSS [15] were prepared according to the literature method. Trisilanol vinylhexaisobutyl-IC-POSS (**2**) was synthesized according to our previous method [37]. Tris(dimethylphenylsilyl)-heptaisobutyl-IC-POSS (**6**) was obtained according to our previous method [35].

Instruments

Measurement ^{1}H-(400 MHz), ^{13}C-(100 MHz), and ^{29}Si-(80 MHz) nuclear magnetic resonance (NMR) spectra were recorded on a Bruker DPX400 spectrometer (Bruker Biospin GmbH, Rheinstetten, Germany). The following abbreviations are used: s, singlet; d, doublet; t, triplet; q, quartet; sep, septet; m, multiplet; br, broad. Fourier transform infrared (FT-IR) spectra were obtained on a JASCO FT/IR-4600 (JASCO, Tokyo, Japan) spectrometer. Gel permeation chromatography (GPC) was performed using a Shimadzu LC-6AD (Shimadzu, Kyoto, Japan) with a Shodex KF-803 column (Showa Denko, Tokyo, Japan). Tetrahydrofuran (THF) was used as an eluent at a flow rate of 1.0 mL/min. Polystyrene (PS) standards were used to calibrate the GPC system. Preparative GPC for purification was performed on a LC-6AD (Shimadzu, Kyoto, Japan) with a Shodex K-2001 (Showa Denko, Tokyo, Japan) and a Shodex K-2002 (Showa Denko, Tokyo, Japan) using chloroform as an eluent. Ultraviolet–visible spectra were recorded on a Jasco spectrophotometer V-670 KKN (Jasco, Tokyo, Japan). Differential scanning calorimetry (DSC) was recorded on a DSC-60 Plus (Shimadzu, Kyoto, Japan). Thermogravimetric analysis (TGA) was performed on a DTA-60 (Shimadzu, Kyoto, Japan) under N$_2$. Powder X-ray diffraction (XRD) was performed on a Rigaku Smartlab X-ray diffractometer with Cu Kα radiation ($\lambda = 1.5406$ Å) in $2\theta/\theta$ mode at room temperature. The 2θ scan data were collected at $0.01°$ intervals at a scan speed of $10°$ (2θ)/min. Ellipsometric analyses were performed on a Film Evaluation System FE-5000S (Otsuka Electronics Co., Ltd.). Measurements were taken at three incidence angles of $70°$. The ellipsometric angles were recorded over a wavelength range of 300–800 nm. High-resolution mass spectra (HRMS) were obtained on a JEOL JMS-SX102A spectrometer. Supercritical fluid chromatography (SFC)–photodiode array (PDA)–mass spectral (MS) analysis was performed on a

Nexera UC system with SPD-M20A and LCMS-8050 (Shimadzu, Kyoto, Japan).

Synthesis

Tris(dimethylsilyl)-*p*-vinylhexaisobutyl-IC-POSS (3)

A dry THF solution (16 ml) of **2** (1.256 g, 1.65 mmol) and triethylamine (2.30 ml, 16.5 mmol) was cooled to 0 °C under N_2 atmosphere, to which chlorodimethylsilane (0.81 ml, 7.42 mmol) was slowly added. After stirring at 0 °C for 1 h and subsequently at room temperature for 3 h, distilled water was added to quench the reaction. The volatile components were evaporated, and the residue was extracted with *n*-hexane. The combined organic layers were dried over $MgSO_4$. After filtration, the volatile components were evaporated. The residue was purified by preparative gel permeation chromatography (GPC) to obtain a colorless solid (0.843 g, 0.901 mmol, 54.6%). ^{1}H-NMR (CDCl$_3$): δ 6.12–5.83 (m, Si–C*H*=C*H*$_2$, 2.68H), 4.77–4.71 (m, Si*H*, 2.38H), 1.90–1.79 (m, –CH$_2$C*H*(CH$_3$)$_2$, 6H), 0.98–0.93 (m, –CH$_2$CH(C*H*$_3$)$_2$, 36H), 0.63–0.52 (m, –C*H*$_2$CH(CH$_3$)$_2$, 12H), and 0.25–0.21 (m, SiH(C*H*$_3$)$_2$, 15.3H). ^{29}Si-NMR (CDCl$_3$): δ –5.4, –67.1, –67.6, –68.0, and –79.7. HR-FAB-MS (*m/z*): calcd for [M]$^+$, 934.3186; obs, 934.3160.

Tris(dimethylphenylsilyl)-*p*-vinylhexaisobutyl-IC-POSS (5)

A dry THF solution (10 ml) of **2** (0.769 g, 1.01 mmol) and triethylamine (1.41 ml, 10.1 mmol) was cooled to 0 °C under N_2 atmosphere, to which chlorodimethylphenylsilane (0.75 ml, 4.54 mmol) was slowly added. After stirring at 0 °C for 1 h and subsequently at room temperature for 3 h, distilled water was added to quench the reaction. The volatile components were evaporated, and the residue was extracted with *n*-hexane. The combined organic layers were dried over $MgSO_4$. After filtration, the volatile components were evaporated. The residue was purified by preparative GPC to obtain a colorless solid (0.721 g, 0.619 mmol, 61.3%). ^{1}H-NMR (CDCl$_3$): δ 7.63–7.55 and 7.37–7.30 (m, Si-*Ph*, 11.98H), 6.14–5.80 (m, Si–C*H*=C*H*$_2$, 2.15H), 1.92–1.79 (m, –CH$_2$C*H*(CH$_3$)$_2$, 6H), 1.01–0.93 (m, –CH$_2$CH(C*H*$_3$)$_2$, 36H), 0.62–0.54 (m, –C*H*$_2$CH(CH$_3$)$_2$, 12H), and 0.43–0.32 (m, SiH(C*H*$_3$)$_2$, 14.6 H). ^{29}Si-NMR (CDCl$_3$): δ –0.9, –67.5, –67.6, and –80.5.

Hyperbranched polymer (7a)

A toluene solution (2 ml) of **3** (0.197 g, 0.211 mmol) and Pt(dvs) (0.1 M in xylene, 10 μl) was stirred at 80 °C overnight under N_2 atmosphere. After the reaction, the volatile components were evaporated. The residue was purified by preparative GPC to obtain a colorless solid (0.121 g,

61.3%). ^{1}H-NMR (in CDCl$_3$, 400 MHz): δ 4.77–4.72 (br, Si*H*, 1.32H), 1.90–1.77 (br, –CH$_2$C*H*(CH$_3$)$_2$, 6H), 0.97–0.93 (br, –CH$_2$CH(C*H*$_3$)$_2$, 36H), 0.63–0.52 (br, –C*H*$_2$CH(CH$_3$)$_2$ and Si–C*H*$_2$–C*H*$_2$–Si, 15H), 0.22–0.19 (br, SiH(C*H*$_3$)$_2$, 9.6H), and 0.15–0.10 (br, CH$_2$–Si(C*H*$_3$)$_2$, 5.3H). ^{29}Si-NMR (CDCl$_3$): δ 10.0, –5.6, –67.2, –67.7, and –67.9.

Post functionalization (7b, 7c)

A toluene solution (2 ml) of **7a** (0.199 g, 0.212 mmol for **7b** and 0.199 g, 0.213 mmol for **7c**) and Pt(dvs) (0.1 M in xylene, 10 μl) was stirred at 80 °C under N_2 atmosphere. After stirring overnight, 2 molar equivalents of the reagent (3-methyl-3-buten-1-ol (**8**) for **7b** and allylheptaisobutyl-T$_8$ cage (**9**) for **7c**) were added to the solution and stirred again. After stirring for 7 h, the volatile components were removed under reduced pressure. The residue was purified by preparative GPC to obtain a colorless solid (0.157 g, 70.5% for **7b** and 0.319 g, 72.4% for **7c**).

For 7b ^{1}H-NMR (in CDCl$_3$, 400 MHz): δ 3.84–3.61 (br, –C*H*$_2$OH, 2.24H), δ 1.89–1.78 (br, –CH$_2$C*H*(CH$_3$)$_2$, –CH$_2$O*H*, and –CH$_2$–C*H*CH$_3$–CH$_2$– 7.8H), 1.50–1.41 (br, –CHCH$_3$–C*H*$_2$–CH$_2$–, 2.33H), 0.97–0.90 (b, –CH$_2$CH(C*H*$_3$)$_2$ and –CH$_2$–CHC*H*$_3$–CH$_2$– 42.4H), 0.67–0.49 (b, –C*H*$_2$CH(CH$_3$)$_2$, –Si–C*H*$_2$–CHCH$_3$–, and –Si–C*H*$_2$–C*H*$_2$–Si–, 18.1H), and 0.20–0.05 (b, –CH$_2$–Si(C*H*$_3$)$_2$, 14.8H). ^{29}Si-NMR (CDCl$_3$): δ 8.8, –67.1~67.9.

For 7c ^{1}H-NMR (in CDCl$_3$, 400 MHz): δ 1.90–1.79 (br, –CH$_2$C*H*(CH$_3$)$_2$, 14.8H), 1.48–1.41 (b, –CH$_2$–C*H*$_2$–CH$_2$–, 2.22H), 0.98–0.93 (b, –CH$_2$CH(C*H*$_3$)$_2$, 89.5H), 0.67–0.52 (b, –C*H*$_2$CH(CH$_3$)$_2$, –Si–C*H*$_2$–C*H*$_2$–Si–, and –Si–C*H*$_2$–C*H*$_2$–C*H*$_2$–Si–, 37.2H), and 0.19–0.05 (b, –CH$_2$–Si(C*H*$_3$)$_2$, 14.8H). ^{29}Si-NMR (CDCl$_3$): δ 8.7, –67.2~68.1, –67.8, and –67.9.

Results and discussion

Synthesis of the AB$_3$-type IC-POSS monomer

Trisilanol vinylhexaisobutyl-IC-POSS (**2**) was prepared from vinylheptaisobutyl-POSS (**1**) according to our previous report [37], which was corner-cleaved by an equimolar amount of aqueous tetraethylammonium hydroxide (TEAOH) at room temperature for 6 h in THF. The three silanol groups of **2** reacted with chlorodimethylsilane to obtain tris(dimethylsilyl)-*p*-vinylhexaisobutyl-IC-POSS (**3**) (Scheme 1). The resultant solid was purified by fractionation with gel permeation chromatography to remove oligomeric parts and obtained a sticky solid in 55% yield. The purity of the product was confirmed by GPC analysis,
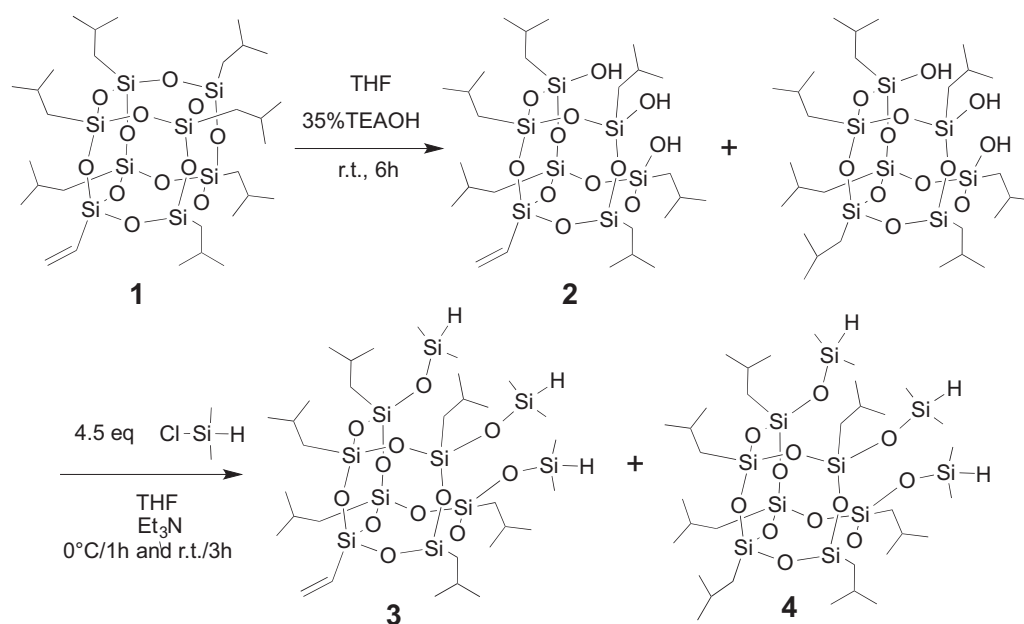
Scheme 1 Synthetic route for tris(dimethylsilyl)-*p*-vinylhexaisobutyl-IC-POSS (**3**)

showing no high-molecular-weight shoulder peak (Figure S1). The AB$_3$-type IC-POSS monomer was soluble in CHCl$_3$, THF, *n*-hexane, ethyl acetate, and toluene and insoluble in methanol.

The structure of **3** was confirmed by FT-IR, ^{1}H-NMR, and ^{29}Si-NMR and HR-FAB-MS analyses. The FT-IR spectrum of **3** shows the disappearance of the Si–OH stretching peak after the capping reaction of **2** (Figure S2). The ^{1}H-NMR spectrum of **3** shows signals corresponding to the vinyl and Si–H groups, as well as the isobutyl and methyl groups, suggesting the successful formation of the AB$_3$-type structure (Fig. 1a). However, the integral ratio of the vinyl and Si–H groups against the isobutyl groups in the ^{1}H-NMR spectrum was rather small compared with the theoretical value (see "Experimental" section). The ^{29}Si-NMR analysis showed a peak at −79.8 ppm, corresponding to the Si atom attached to the vinyl group, and a signal at −5.4 ppm, corresponding to the dimethylsilyl unit. In addition to two signals at −67.6 ppm and −68.0 ppm, corresponding to the Si atoms attached to the isobutyl group, a signal at −67.1 ppm was observed, suggesting the contamination of tris(dimethylsilyl)-heptaisobutyl-POSS (**4**) (Fig. 1b). The HR-FAB-MS result provided conclusive evidence for the formation of the expected structure. In addition, other peaks corresponding to **4** were also detected. The integral ratio in the ^{1}H-NMR spectrum suggests that the content of **4** in **3** is 9.3 mol%. This minor product was produced from trisilanol heptaisobutyl-IC-POSS, which was obtained as a by-product through the removal of the vinyl-substituted corner of **1** (Scheme 1).

Contamination of **4** was further confirmed by SFC-PDA-MS analysis. For detection with a UV detector, the three

silanol groups of **2** reacted with chlorodimethylphenylsilane instead of chlorodimethylsilane to obtain tris(dimethylphenylsilyl)-*p*-vinylhexaisobutyl-IC-POSS (**5**). Tris(dimethylphenylsilyl)-heptaisobutyl-IC-POSS (**6**) was also prepared to confirm contamination of the minor product in the AB$_3$-type IC-POSS monomer. Although the UV chromatograph hardly detected the contamination of **6** in **5**, the MS detector clearly showed fractions corresponding to both **6** and **5**, confirming that the AB$_3$-type IC-POSS monomer **6** was contaminated in sample **5** (Figure S3).

Polymerization

Since separation of the AB$_3$-type POSS monomer, tris(dimethylsilyl)-*p*-vinylhexaisobutyl-IC-POSS (**3**), from **4** as the B$_3$-type monomer failed, we used the AB$_3$-type IC-POSS monomer containing 12.5 mol% of **4** for polymerization. We studied the hydrosilylation polymerization of **3** as the AB$_3$-type IC-POSS monomer in the presence of Karstedt's catalyst in toluene at 80 °C overnight (Scheme 2). After purification by preparative GPC, sticky polymeric products (**7a**) were obtained. The obtained polymer was soluble in organic solvents such as acetone, *n*-hexane, toluene, CHCl$_3$, and THF. The GPC analysis (THF, PSt standards) of **7a** showed that the number average molecular weight (M_n) and molecular weight distribution (M_w/M_n) of the polymer are 3.9×10^3 and 1.39, respectively (Fig. 2).

The chemical structure of the polymer was characterized by ^{1}H-NMR, ^{29}Si-NMR, and FT-IR. The FT-IR spectrum showed a peak for Si–O–Si stretching, supporting the cage silsesquioxane structure (Figure S4). The ^{1}H-NMR spectrum

Fig. 1 a ^{1}H- and **b** ^{29}Si-NMR spectra of **3** in CDCl$_3$
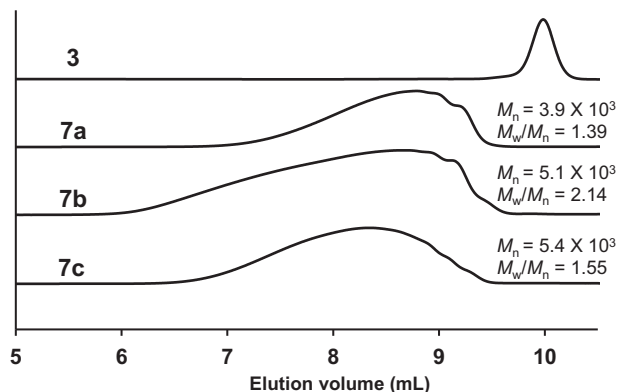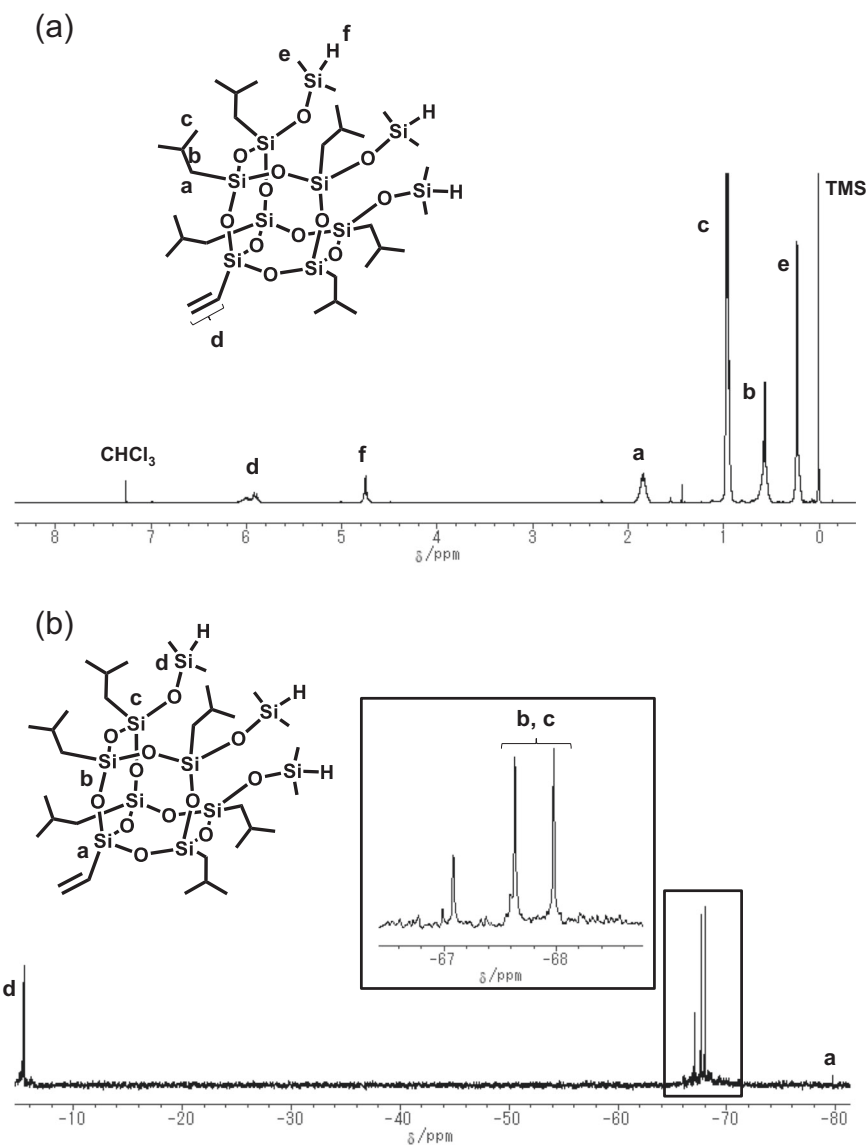

(a)

(b)

Fig. 2 GPC traces of **3**, **7a**, **7b**, and **7c** using THF as an eluent with RI detection

is in agreement with the proposed structure (Figure S5). The peak corresponding to the vinyl group disappeared, and the peak at 4.74 ppm, corresponding to the SiH group, decreased. The integral ratio of the Si–H groups against the isobutyl groups in the ^{1}H-NMR spectrum suggests that 45% of the Si–H groups reacted. The ^{29}Si-NMR analysis showed peaks at 10 ppm and −5.4 ppm, corresponding to Si–CH$_2$–CH$_2$–Si and SiH(CH$_3$)$_2$, respectively (Figure S6). The degree of branching of the HB polymer was poorly estimated, as dendritic, semi-dendritic, and linear units in the present HB polymer could hardly be distinguished in the ^{1}H- and ^{29}Si-NMR spectra.

Post functionalization

The resulting HB polymer, which had a number average molecular weight (M_n) of 3.9×10^3, and terminal Si–H
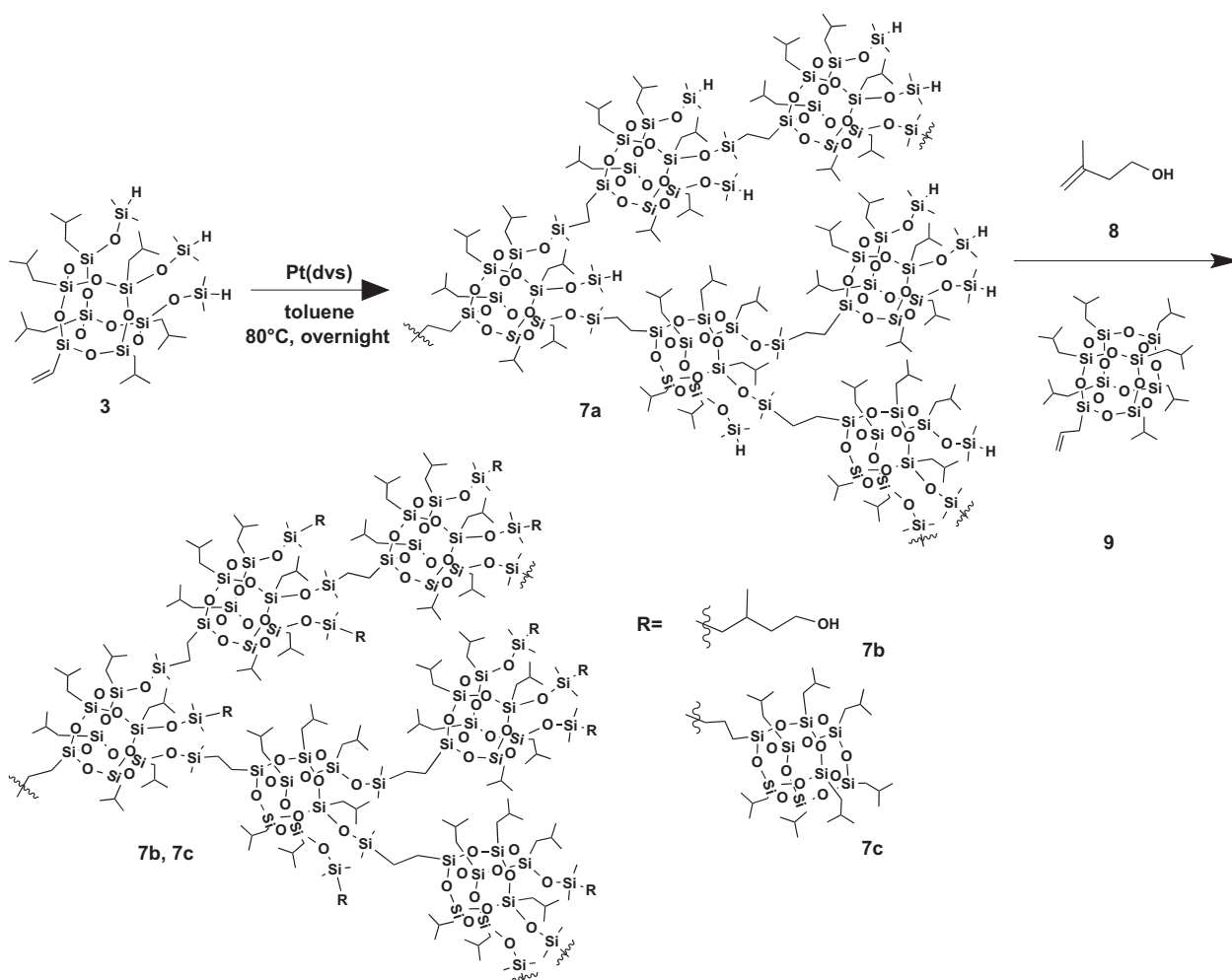
Scheme 2 Hydrosilylation polymerization of **3** and post functionalization with isoprenol (**8**) or allylheptaisobutyl-POSS (**9**)

groups, reacted with two molar equivalents of isoprenol (**8**) or allylheptaisobutyl-POSS (**9**) against the Si–H groups in the presence of Karstedt's catalyst in toluene at 80 °C for 7 h (Scheme 2). After purification by preparative GPC, polymeric products with isoprenol or allylheptaisobutyl-POSS (**7b** and **7c**, respectively) were obtained in yields of 70% and 72%, respectively. All the HB polymers were soluble in hydrophobic organic solvents such as $CHCl_3$, THF, *n*-hexane, ethyl acetate, and toluene. Although the SiH- and allylheptaisobutyl-POSS-terminated HB polymers, **7a** and **7c**, were insoluble in methanol, the isoprenol-terminated HB polymer (**7b**) formed a cloudy solution. Introducing the hydroxyl group on the terminus of the HB polymer increased the dispersibility in polar organic solvents.

After post functionalization, the peaks corresponding to the Si–H group disappeared in the ^{1}H-NMR spectra of both samples, indicating that all the Si–H groups were hydrosilylated with isoprenol or allylheptaisobutyl-POSS (Figures S7 and S9). The integral ratio of the methine protons of the isobutyl units against the α-methylene protons of the hydroxyl units suggests that the functionalization ratio of isoprenol against the Si–H group was 85%. The integral ratio of the methine protons of the isobutyl units against the β-methylene protons of the linker units suggests that the functionalization ratio of allylheptaisobutyl-POSS against the Si–H group was 83%. The ^{29}Si-NMR analysis of **7b** and **7c** showed the disappearance of the peak at −5.4 ppm, corresponding to $SiH(CH_3)_2$, while the peak at 10 ppm, corresponding to $Si–CH_2–CH_2–Si$, remained (Figures S8 and S10). GPC analysis (THF, PSt standards) of **7b** and **7c** shows that the introduction of isoprenol increased the M_n from 3.9×10^3 to 5.1×10^3, while introduction of the allylheptaisobutyl-T_8 cage slightly increased the M_n to 5.4×10^3 compared with that of the isoprenol-terminated HB polymer, even when large amounts of POSS units were introduced into the HB polymer (Fig. 2). This observation suggests that the HB polymer terminated with allylheptaisobutyl-POSS had a compact structure in the solution.

Thermal and optical properties

The HB polymer before post functionalization showed 1% and 5% weight loss at 298 and 355 °C, respectively, under N_2 (Fig. 3). After the introduction of isoprenol and allyl-heptaisobutyl-POSS, the polymers showed 1% weight loss at 285 and 358 °C, respectively, under N_2. Introducing POSS units at the terminus significantly increased the thermal stability. Differential scanning calorimetry (DSC) showed that the glass-transition temperatures of the iso-prenol- and allylheptaisobutyl-POSS-terminated HB polymers were observed at 21 and −13 °C, respectively (Fig. 4). The glass-transition temperature of the unmodified HB polymer may be lower than −50 °C.
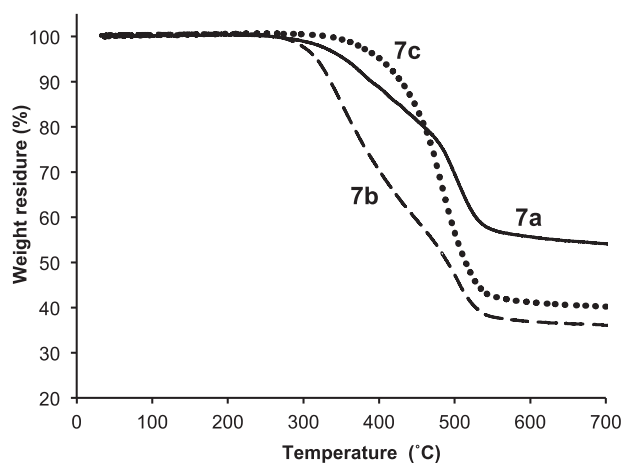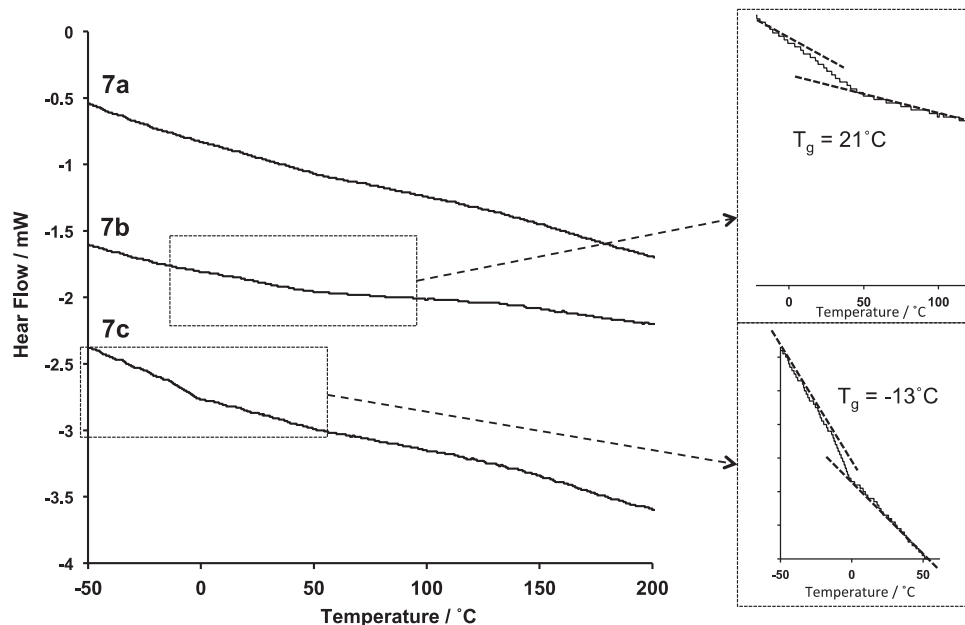

Fig. 3 TGA curves of **7a**, **7b**, and **7c** under N_2

A THF solution of the polymers was cast on a glass substrate. The film showed excellent transparency in the visible region (Fig. 5). The optical transmittance of the colorless films, with a film thickness of 0.1 mm, of all the polymers was over 90% in the visible region between 780 and 380 nm. The refractive index of the unmodified polymer film was 1.4376. Post functionalization with isoprenol and allylheptaisobutyl-POSS increased the refractive index to 1.4464 and 1.4573, respectively. The HB polymers are good candidates for lower-density polymers because of their three-dimensional globular architectures with highly branched structures.

The XRD pattern of the polymer shows a broad peak centered at a 2θ value of 18°, indicating an amorphous polymer (Fig. 6). The polymer also shows a broad diffraction peak at a 2θ value of ~8°. The spacing evaluated from the 2θ value was 1.10 nm, corresponding to the isobutyl-substituted IC-POSS unit. Peaks for SiH-, isoprenol-, and allylheptaisobutyl-POSS-terminated HB polymers were observed at 8.23, 7.99, and 8.28, respectively. The spacing values determined from the peak positions were 1.07, 1.11, and 1.07 nm, respectively, corresponding to the cage sil-sesquioxane unit. The packing structure of the isoprenol-terminated HB polymer was expanded. In contrast, a denser structure was formed for the allylheptaisobutyl-POSS-terminated HB polymer.

Conclusions

Here, we prepared an incompletely condensed cage silsesquioxane-based AB_3-type monomer, tris(dimethylsi-lyl)-*p*-vinylhexaisobutyl-IC-POSS (**3**), by the corner-
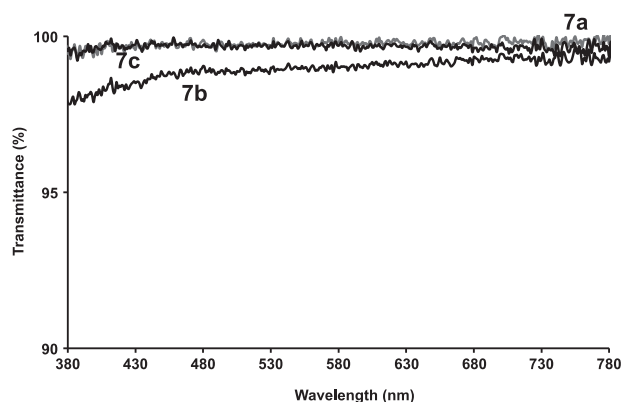

Fig. 4 DSC curves of **7a**, **7b**, and **7c**

Fig. 5 UV-vis spectra of the films obtained from **7a**, **7b**, and **7c** on soda lime glass. The thickness was ~0.1 μm
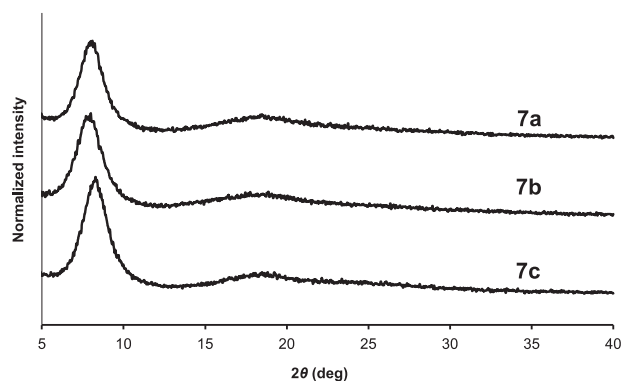

Fig. 6 XRD profiles of **7a**, **7b**, and **7c**

cleaved reaction of vinylheptaisobutyl-POSS (**1**) and subsequent capping reaction with chlorodimethylsilane. Although 12.5 mol% tris(dimethylsilyl)-heptaisobutyl-IC-POSS (**4**), which was produced by the corner-cleaved reaction of **1**, was contaminated in **3**, as estimated by analytical methods, the hydrosilylation polymerization of **3** provided a soluble polymer, with a number average molecular weight (M_n) and molecular weight distribution (M_w/M_n) of 3.9×10^3 and 1.39, respectively. The refractive index of the unmodified polymer film was 1.4376. Post functionalization with isoprenol increased the dispersibility in polar organic solvents and significantly increased the glass-transition temperature. Post functionalization with allylheptaisobutyl-POSS significantly increased the thermal stability due to the denser structure, as supported by XRD analysis. Their refractive index varied from 1.4464 to 1.4573 upon post functionalization. The properties of HB polymers are extremely dependent on the terminal functional groups and can be tailored by chemical modification [38, 39].

Compliance with ethical standards

Conflict of interest The authors declare that they have no conflict of interest.

References

1. Lichtenhan JD, Otonari YA, Cam MJ. Linear hybrid polymer building blocks: methacrylate-functionalized polyhedral oligomeric silsesquioxane monomers and polymers. Macromolecules. 1995;28:8435–7.
2. Zheng L, Hong S, Cardoen G, Burgaz E, Gido SP, Coughlin EB. Polymr nanocomposites through controlled self-assembly of cubic silsesquioxane scaffolds. Macromolecules. 2004;37:8606–11.
3. Ahn B, Hirai T, Jin S, Rho Y, Kim K-W, Kakimoto M, Gopalan P, Hayakawa T, Ree M. Hierachical structure in nanoscale thin films of a poly(styrene-*b*-mehtacrylate grafted with POSS) (PS$_{214}$-*b*-PMAPOSS$_{27}$). Macromolecules. 2010;43:10568–81.
4. Wu J, Ge Q, Mather PT. PEG-POSS multiblock polyurethanes: synthesis, characterization, and hydrogel formation. Macromolecules. 2010;43:7637–49.
5. Lee J, Cho H-J, Jung B-J, Cho NS, Shim H-K. Stabilized blue luminescent polyfluorenes: Introducing polyhedral oligomeric silsesquioxane. Macromolecules. 2004;37:8523–9.
6. Pyun J, Matyjaszewski K. The synthesis of hybrid polymers using atom transfer radical polymerization: homopolymers and block copolymers from polyhedral oligomeric silsesquioxane monomers. Macromolecules. 2000;33:217–20.
7. Escudé NC, Chen EY-X. Stereoregular methacrylate-POSS hybrid polymers: synthesis and nanostructured assemblies. Chem Mater. 2009;21:5743–4.
8. Higashihara T, Segawa Y, Sinanawanich W, Ueda M. Synthesis of hyperbranched polymers with controlled degree of branching. Polym J. 2012;44:14–29.
9. Voit BI, Lederer A. Hyperbranched and highly branched polymer architectures—synthesis strategies and major characterization aspects. Chem Rev. 2009;109:5924–73.
10. Voit B. Hyperbranched polymers—all problems solved after 15 years of research? J Polym Sci Part A. 2005;43:2679–99.
11. Kim YH. Hyperbranched polymers 10 years after. J Polym Sci Polym Chem Ed. 1998;36:1685–98.
12. Haldar U, Roy SG, De P. POSS tethered hybrid "inimer" derived hyperbranched and star-shaped polymers via SCVP-RAFT technique. Polymer. 2016;97:113–21.
13. Chang Y-T, Shu C-F, Leu C-M, Wei K-H. Synthesis and characterization of hyperbranched aromatic poly(ether imide)s with terminal amino groups. J Polym Sci Part A Polym Chem. 2003;41:3726–35.
14. Wang J, Ye Z, Joly H. Synthesis and characterization of hyperbranched polyethylenes tethered with polyhedral oligomeric silsesquioxane (POSS) nanoparticles by chain walking ethylene copolymerization with acryloisobutyl-POSS. Macromolecules. 2007;40:6150–63.
15. Seino M, Hayakawa T, Ishida Y, Kakimoto M. Synthesis and characterization of crystalline hyperbranched polysiloxylsilane with POSS groups at the terminal position. Macromolecules. 2006;39:8892–4.
16. Xu N, Stark EJ, Dvornic PR, Meier DJ, Hu J, Hartmann-Thompson C. Hyperbranched polycarbosiloxanes and polysiloxanes with octafunctional polyhedral oligomeric solsesquioxane (POSS) branch points. Macromolecules. 2012;45:4730–9.
17. Li D, Niu Y, Yang Y, Wang X, Yang F, Shen H, Wu D. Synthesis and self-assembly behavior of POSS-embedded hyperbranched polymers. Chem Commun. 2015;51:8296–9.

18. Xu N, Stark EJ, Carver PI, Sharps P, Hu J, Hartmann-Thompson C. Hyperbranched polyhedral oligomeric silsesquioxane (HB-POSS) nanomaterials for high transmission and radiation-resistant space and solar application. J Appl Polym Sci. https://doi.org/10.1002/APP.39418 (2013).

19. Miyasaka M, Fujiwara Y, Kudo H, Nishikubo T. Synthesis and characterization of hyperbranched polymer containing of silsesquioxane derivatives. Polym J. 2010;42:799–803.

20. Cordes DB, Lickiss PD, Rataboul F. Recent developments in the chemistry of cubic polyhedral oligosilsesquioxanes. Chem Rev. 2010;110:2081–173.

21. Irie Y, Naka K. Synthesis of imidazole-terminated hyperbranched polymers with POSS-branching points and their pH responsive and coordination properties. J Polym Sci Part A Polym Chem. 2013;51:2696–701.

22. Seino M, Hayakawa T, Ishida Y, Kakimoto M, Watanabe K, Oikawa H. Hydrosilylation polymerization of double-decker-shaped silsesquioxane having hydrosilane with diynes. Macromolecules. 2006;39:3473–5.

23. Wu S, Hayakawa T, Kikuchi R, Grunzinger SJ, Kakimoto M. Synthesis and characterization of semiaromatic polyimides containing POSS in main chain derived from double-decker-shaped silsesquioxane. Macromolecules. 2007;40:5698–705.

24. Yoshimatsu M, Komori K, Ohnagamitsu Y, Sueyoshi N, Kawashima N, Chinen S, Murakami Y, Izumi J, Inoki D, Sakai K, Matsuo T, Watanabe K, Kunitake M. Necklace-shaped dimethylsiloxane polymers bearing a polyhedral oligomeric silsesquioxane cage prepared by polycondensation and ring-opening polymerization. Chem Lett. 2012;41:622–4.

25. Pinson DM, Yandek GR, Haddad TS, Horstman EM, Mabry JM. Thermosetting poly(imide silsesquioxane)s featuring reduced moisture affinity and improved processability. Macromolecules. 2013;46:7363–77.

26. Feher FJ, Newman DA, Walzer JF. Silsesquioxanes as modles for silica surfaces. J Am Chem Soc. 1989;111:1741–8.

27. Lichtenhan JD, Vu NQ, Carter JA, Gilman JW, Feher FJ. Silsesquioxane-siloxane copolymers from polyhedral silsesquioxanes. Macromolecules. 1993;26:2141–2.

28. Wright ME, Schorzman DA, Feher FJ, Jin R-Z. Synthesis and thermal curing of aryl-ethynyl-terminated coPOSS imide oligomers: new in organic/organic hybrid resins. Chem Mater. 2003;15:264–8.

29. Feher FJ, Terroba R, Ziller JW. A new rout to incompletely-condensed silsesquioxanes: base-mediated cleavage of polyhedral oligosilsesquioxanes. Chem Commun. 1999;35:2309–10.

30. Raftopoulos KN, Jancia M, Aravopoulou D, Hebda E, Pielichowski K, Pissis P. POSS along the hard segments of polyurethane. Phase separation and molecular dynamics. Macromolecules. 2013;46:7378–86.

31. Carniato F, Boccaleri E, Marchese L. A versatile rout to bifunctionalized silsesquixane (POSS): synthesis and characterization of Ti-containing aminopropylisobutyl-POSS. Dalton Trans. 2008;37:36–39.

32. Olivero F, Renò F, Carniato F, Rizzi M, Cannas M, Marchese L. A novel luminescent bifunctional POSS as a molecular platform for biomedical applications. Dalton Trans. 2012;41:7467–73.

33. Wang X-M, Guo Q-Y, Han S-Y, Wang J-Y, Han D, Fu Q, Zhang W-B. Stochastic/controlled symmetry breaking of the T8-POSS cages towards multifunctional regioisomeric nanobuildlig blocks. Chem Eur J. 2015;21:1–11.

34. Han S-Y, Wang X-M, Shao Y, Guo Q-Y, Li Y, Zhang W-B. Janus POSS based on mixed [2:6] octakis-adduct regioisomers. Chem Eur J. 2016;22:6397–403.

35. Imoto H, Nakao Y, Nishizawa N, Fujii S, Nakamura Y, Naka K. Tripodal polyhedral oligomeric silsesquioxanes as novel class of three-dimensional emulsifiers. Polym J. 2015;47:609–15.

36. Yuasa S, Sato Y, Imoto H, Naka K. Fabrication of composite films with poly(methyl methacrylate) and incompletely condensed cage-silsesquioxane fillers. J Appl Polym Sci. https://doi.org/10.1002/app.46033 (2017).

37. Maegawa T, Irie Y, Imoto H, Fueno H, Tanaka K, Naka K. para-Bisvinylhexaisobutyl-substituted T_8 caged monomer: synthesis and hydrosilylation polymerization. Polym Chem. 2015;6:7500–4.

38. Zak P, Pietraszuk C, Marciniec B, Spólnik G, Danikiewicz W. Efficient functionalization of cubic monovinylsilsesquioxanes via cross-metathesis and silylative coupling with olefins in the presence of ruthenium complexes. Adv Synth Catal. 2009;351:2675–82.

39. Yasumoto Y, Yamanaka T, Sakurai S, Imoto H, Naka K. Design of low-crystalline and -density isobutyl-substituted caged silsesquioxane derivatives by star-shaped architectures linked with short aliphatic chains. Polym J. 2016;48:281–7.